Estimation of sensitivity for the OST transit spectrograph

Shohei Goda (Osaka University)

Set of parameters

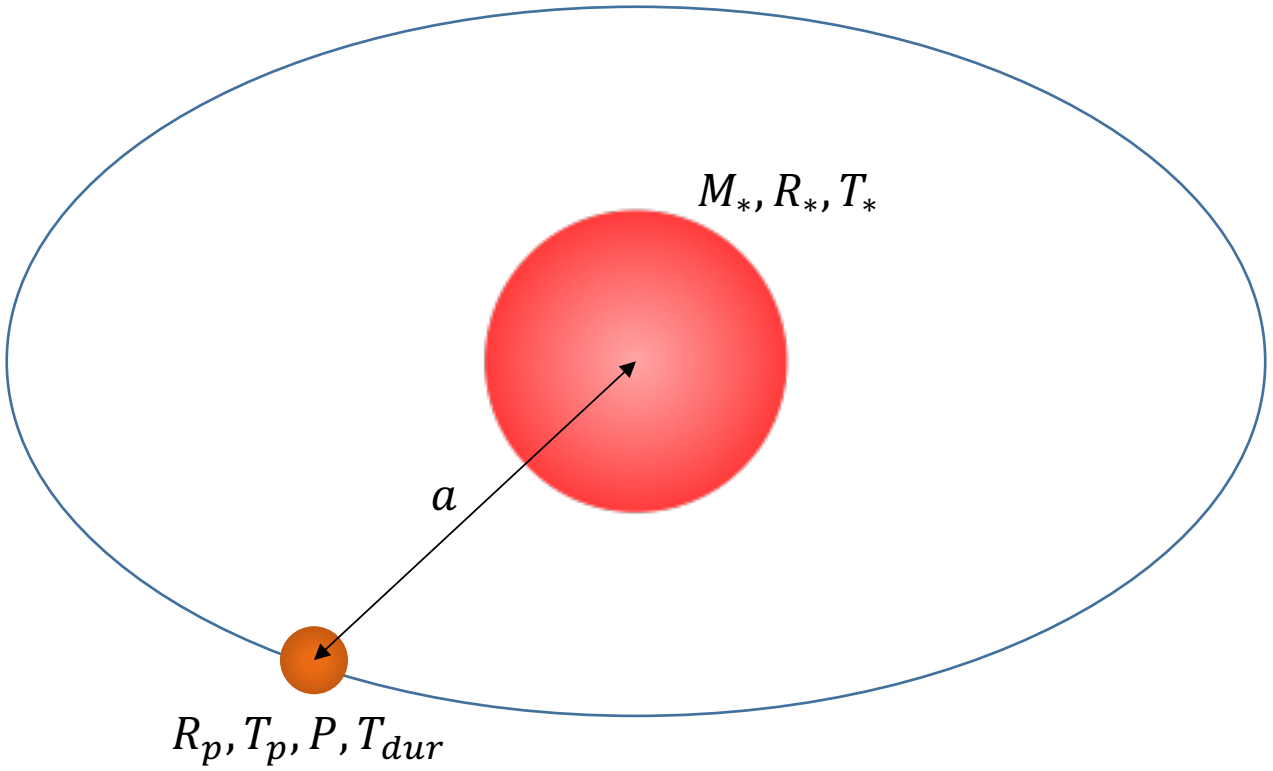

$$R_*(R_\odot) = -10.8828(\pm 0.1355) + 7.18727(\pm 0.09468)\times 10^{-3} T_* - 1.50957(\pm 0.02155)\times 10^{-6} T_*^2 + 1.07572(\pm 0.01599)\times 10^{-10} T_*^3$$

$$R_*(R_\odot) = 0.0906(\pm 0.0027) + 0.6063(\pm 0.0153) M_* + 0.3200(\pm 0.0165) M_*^2$$

Boyajian et al. 2012

$R_p = R_\oplus$

$T_p = 280K$

$T_{dur} = \frac{2R_*}{2\pi a} P$ (P: Orbital Period)

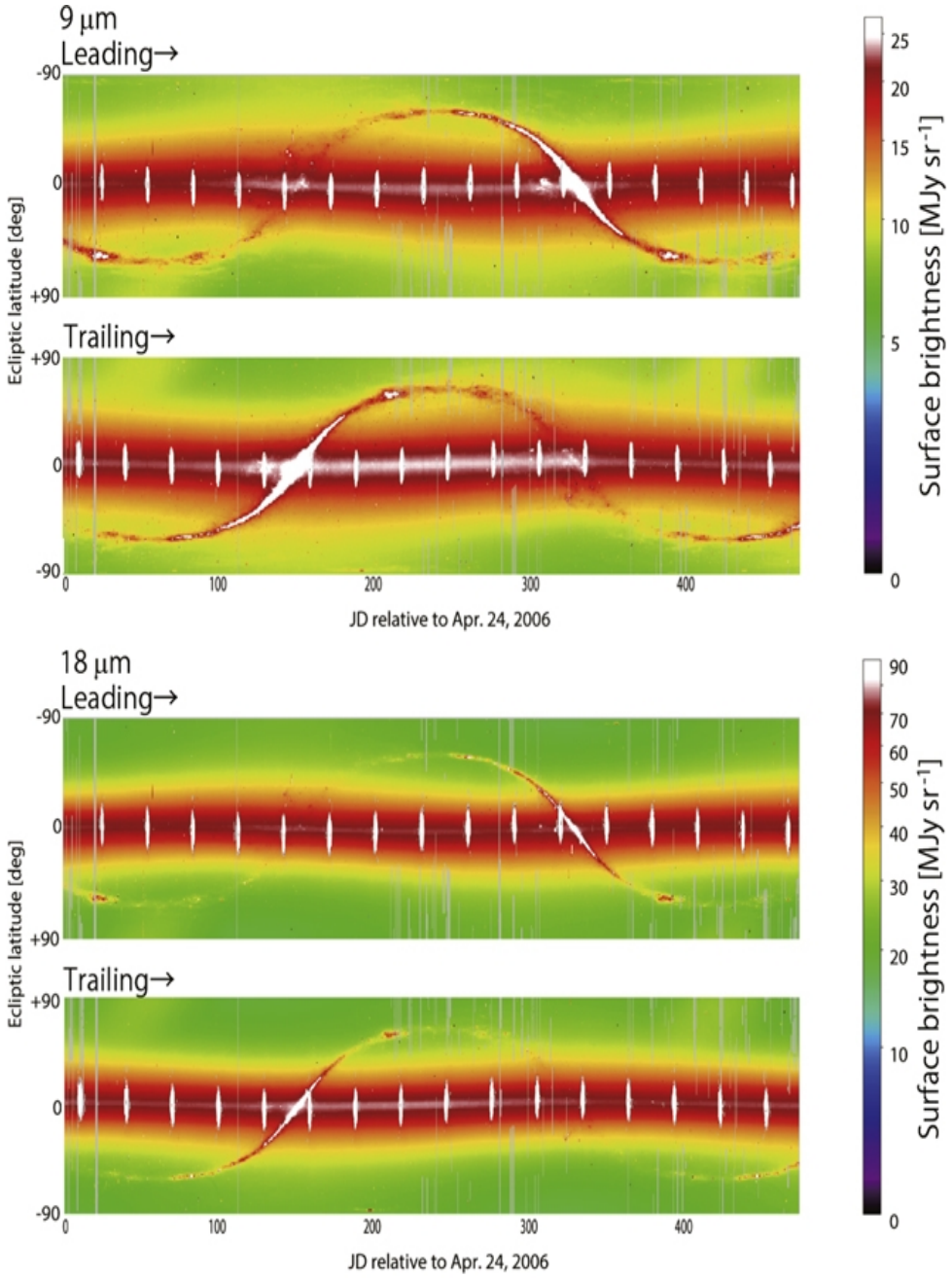

1MJy/steradian
= 2.35E-31 W/m^2/Hz/arcsec^2
= 8.70E-13 W/m^2/m/as^2 (@9μm)
= 8.70E-19 W/m^2/μm/as^2 (@9μm)

Figure 1. *AKARI* mid-IR all-sky diffuse maps on the plane of the ecliptic latitude vs. the Julian day relative to 2006 April 24, where the scan direction is from bottom to top. For each of the 9 and 18 μm maps, the upper and the lower panels correspond to the leading and the trailing sides, respectively. The arrow shown in the top left of each map indicates the direction of the shift of the scan path, which is useful for comparison with the DIRBE maps in Figure 6.

Figure 1 from Modeling of the Zodiacal Emission for the AKARI/IRC Mid-infrared All-sky Diffuse Maps
Toru Kondo et al. 2016 AJ 151 71 doi:10.3847/0004-6256/151/3/71

Table 1
Parameters of the IPD Model in Kelsall et al. (1998) and in the Present Study

Parameter	Name of Parameter	Kelsall et al. (1998)	Present Study
	All cloud components		
T_0 (K)	Temperature at 1 au	286 (fixed)	286 (fixed)
δ	Temperature power-law index	0.467 (0.004)	0.458 (0.006)
$\varepsilon_{9\,\mu m}$	Emissivity modification factor at 9 μm	...	0.8575 (0.0007)
	Smooth cloud		
n_0 (au^{-1})	Density at 1 au	1.134×10^{-7} (0.006×10^{-7})	1.578×10^{-7} (0.006×10^{-7})
α	Radial power-law index	1.34 (0.02)	1.59 (0.02)
β	Vertical shape parameter	4.14 (0.07)	4.85 (0.02)
γ	Vertical power-law index	0.94 (0.03)	1.043 (0.005)
μ	Widening parameter	0.19 (0.01)	0.180 (0.002)
i (deg)	Inclination	2.03 (0.02)	2.047 (0.007)
Ω (deg)	Ascending node	77.7 (0.6)	75.9 (0.1)
X_0 (au)	x offset from the Sun	0.012 (0.001)	0.0153 (0.0002)
Y_0 (au)	y offset from the Sun	0.0055 (0.0008)	−0.0081 (0.0002)
Z_0 (au)	z offset from the Sun	−0.0022 (0.0004)	−0.00160 (0.00004)
	Dust bands		
n_{B1} (au^{-1})	Density at 3 au of band 1	5.6×10^{-10} (0.7×10^{-10})	5.6×10^{-10} (0.1×10^{-10})
n_{B2} (au^{-1})	Density at 3 au of band 2	2.0×10^{-9} (0.1×10^{-9})	3.70×10^{-9} (0.03×10^{-9})
n_{B3} (au^{-1})	Density at 3 AU of band 3	1.4×10^{-10} (0.2×10^{-10})	0.06×10^{-10} (0.05×10^{-10})
	Circumsolar ring		
n_{SR} (au^{-1})	Density at 1 au	1.8×10^{-8} (0.1×10^{-8})	0.75×10^{-8} (0.06×10^{-8})
R_{SR} (au)	Radius of peak density	1.0282 (0.0002)	1.0282 (fixed)
σ_{rSR} (au)	Radial dispersion	0.025 (fixed)	0.025 (fixed)
σ_{zSR} (au)	Vertical dispersion	0.054 (0.007)	0.066 (0.002)
	Earth-trailing blob		
n_{TB} (au^{-1})	Density at 1 au	1.9×10^{-8} (0.1×10^{-8})	2.08×10^{-8} (0.01×10^{-8})
R_{TB} (au)	Radius of peak density	1.06 (0.01)	1.06 (fixed)
σ_{rTB} (au)	Radial dispersion	0.10 (0.01)	0.10 (fixed)
σ_{zTB} (au)	Vertical dispersion	0.09 (0.01)	0.151 (0.001)
θ_{TB} (deg)	Longitude with respect to Earth	−10 (fixed)	−10 (fixed)
$\sigma_{\theta TB}$ (deg)	Longitude dispersion	12 (3)	11.10 (0.06)
$Z_{0,TB}$ (au)	z offset from the Sun	0.0 (fixed)	0.0206 (0.0005)
	Circumsolar ring + Earth-trailing blob		
i_{RB} (deg)	Inclination	0.49 (0.06)	0.97 (0.03)
Ω_{RB} (deg)	Ascending node	22.28 (0.001)	296 (1)
	Constant component		
$C_{9\,\mu m}$ (MJy sr^{-1})	Brightness at 9 μm	...	0.191 (0.004)
$C_{18\,\mu m}$ (MJy sr^{-1})	Brightness at 18 μm	...	0.246 (0.009)

Note. For details of the parameters, see Kelsall et al. (1998). The values in the parentheses indicate 1σ errors.

Inter-Planetary-Disk Model Detail
http://iopscience.iop.org/article/10.1086/306380/fulltext/

Characteristics of the target system

Items	Values
Star	-
Distance (pc)	10 (fixed)
Temperature (K)	2500~4000 (variable)
Limb darkening	None
Planet	-
Inclination (°)	90 (fixed)
Temperature (K)	280 (fixed)
Background	-
Surface brightness at 9μm	5, 10, 20 (variable)
Temperature (K)	275 (fixed)
Spectrum (*)	Black body

(*) Note. The spectrum of background is derived as a black body with temperature of 275K.

Specifications of the OST and its transit spectrograph

Items	Values
OST	-
Primary mirror diameter (cm)	924 (fixed)
Transit spectrograph	-
Number of science pixels	400,000
Number of onboard reference pixels	1,600,000 (*)
Number of outboard reference pixels	2,000,000 (*)
Transmittance inq. QE (%)	10 (fixed)
Range of wavelength (μm)	6~25
Spectral resolution ($\Delta\lambda$)	0.08 (6~10μm), 0.14 (10~18μm), 0.07 (18~25μm)
Exposure time at one time (sec)	60 (fixed)
Field stop radius (arcsec)	1, 2, 4 (variable)

(*) Note. The two types of reference pixels are considered in this calculation (see p.8).

Assumptions of detector noise

Items	Values
Peak-to-peak of gain fluctuation (ppm)	None
Dark current (electron/sec)	0.2 (fixed)
Readout noise (electron/time)	14 (fixed)
Systematic noise	None

Assumption of detector plane

(see also Appendix C of feasibility report)

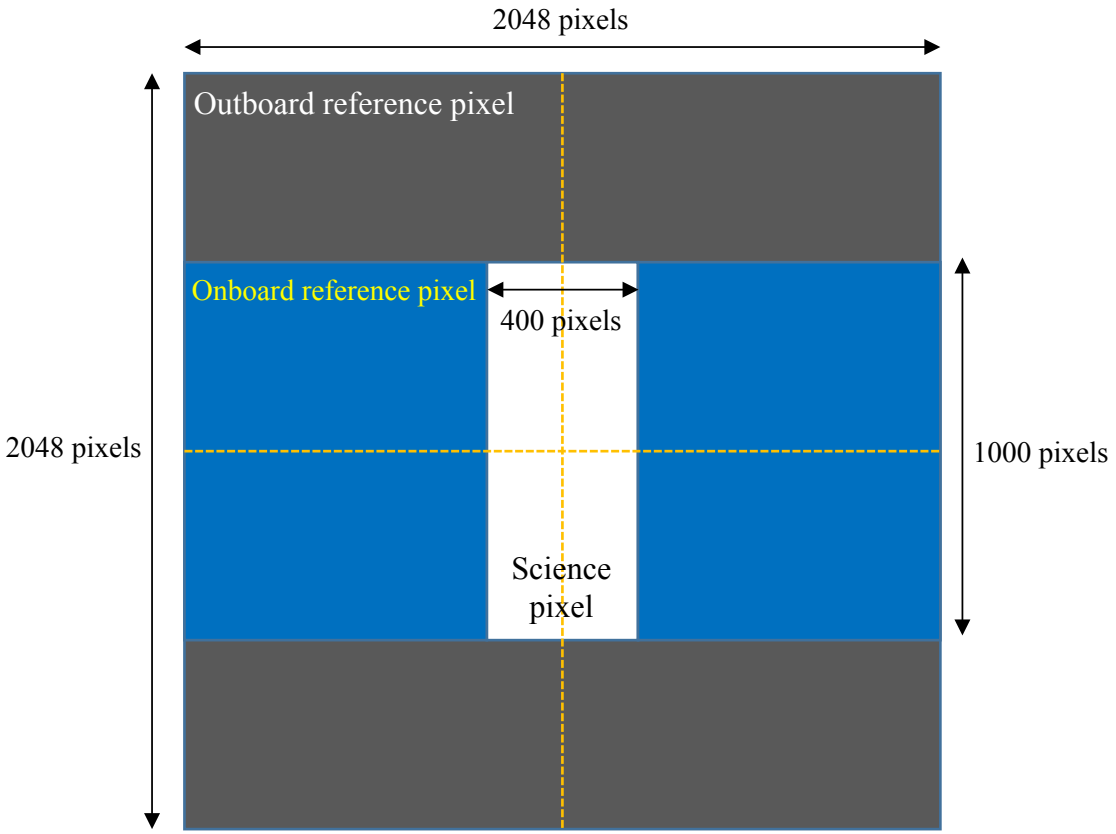

- Configuration of science and two types of reference pixels. The white-, blue-, and black-colored regions represent the science, onboard reference, and outboard reference pixels, respectively.
- While the onboard reference pixel is shielded from any thermal radiation with a cold mask put on the pupil plane, the outboard reference pixel does not apply indium bumping, which connects a Si:As focal plane array with a Si readout integrated circuit (ROIC).
- The numbers of the science, onboard reference, and outboard reference pixels are, respectively, 4×10^5, 1.6×10^6, and 2.0×10^6. Given that vertical stripes are mainly produced by the multiplexers, the outboard reference pixels are arranged horizontally.

Calibration of common-mode noise

- The i-th science, onboard and outboard pixel values with the j-th readout electronics:

$$D_{sci,i,j} = g_j(of_i + Q_i) + V_{i,j} \approx \overline{g_j}\left(o\overline{f_i} + \overline{Q_i}\right) + V_{i,j} + \overline{g_j}o\delta f_i + \underbrace{\left(o\overline{f_i} + \overline{Q_i}\right)\delta g_j}_{\text{Gain fluctuation}} + \sigma_{sci,i,j}$$

$$D_{onref,i,j} = g_j Q_i + V_{i,j} \approx \overline{g_j}\,\overline{Q_i} + V_{i,j} + \underbrace{\overline{Q_i}\delta g_j}_{\text{Gain fluctuation}} + \sigma_{onref,i,j}$$

$$D_{outref,i,j} = V_{i,j} + \sigma_{outref,i,j}$$

- The calibrated science pixel value:

$$D_{sub,i,j} = D_{sci,i,j} - \underbrace{\left(D_{onref,i,j} - \overline{D_{onref,i,j}}\right) \times \frac{\overline{D_{sci,i,j}} - \overline{D_{outref,i,j}}}{\overline{D_{onref,i,j}} - \overline{D_{outref,i,j}}}}_{\text{Subtract the gain fluctuation (next page)}} - \underbrace{\overline{D_{outref,i,j}}}_{\text{Subtract the offset}} \qquad (1)$$

g: Gain
o: Transmittance
f: Star flux
Q: Dark current
V: Offset voltage
σ : Random noise
$A = \bar{A} + \delta A$
$\bar{A}$: Average value
δA: Fluctuation

Calibration of common-mode noise

- The gain fluctuation attached to the science pixels can be estimated from the onboard and outboard reference pixels:

$$\left(D_{onref,i,j} - \overline{D_{onref,i,j}}\right) \times \frac{\overline{D_{sci,i,j}} - \overline{D_{outref,i,j}}}{\overline{D_{onref,i,j}} - \overline{D_{outref,i,j}}} \approx \left(\overline{Q_i}\delta g_j + \sigma_{onref,i,j}\right) \times \frac{o\overline{f_i} + \overline{Q_i}}{\overline{Q_i}}$$

$$= \left(o\overline{f_i} + \overline{Q_i}\right)\delta g_j + \frac{o\overline{f_i} + \overline{Q_i}}{\overline{Q_i}}\sigma_{onref,i,j}$$

- The calibrated science pixels are attached with only the random noise:

$$D_{sub,i,j} = D_{sci,i,j} - \left(D_{onref,i,j} - \overline{D_{onref,i,j}}\right) \times \frac{\overline{D_{sci,i,j}} - \overline{D_{outref,i,j}}}{\overline{D_{onref,i,j}} - \overline{D_{outref,i,j}}} - \overline{D_{outref,i,j}}$$

$$\approx \overline{g_j}\left(o\overline{f_i} + \overline{Q_i}\right) + \overline{g_j}o\delta f_i + \sigma_{sub,i,j}$$

Random noise

Random noise attached to calibrated science pixels

$$\begin{cases} \sigma_{sci,i,j} \approx \sqrt{\overline{g_j} o\overline{f_i} + \overline{g_j}\overline{Q_i} + V_{i,j}} \\ \sigma_{onref,i,j} \approx \sqrt{\overline{g_j}\overline{Q_i} + V_{i,j}} \\ \sigma_{outref,i,j} \approx \sqrt{V_{i,j}} \end{cases}$$

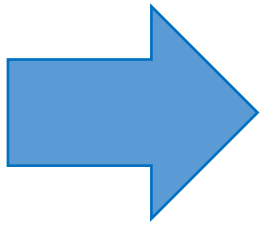

$$\begin{cases} \sigma_{sci,bin} \approx \sqrt{\left(\overline{g_j} o\overline{f_i} + \overline{g_j}\overline{Q_i} + V_{i,j}\right)\times n_{sci}} \\ \sigma_{onref,ave} \approx \sqrt{\dfrac{\overline{g_j}\overline{Q_i} + V_{i,j}}{n_{onref}}} \\ \sigma_{outref,ave} \approx \sqrt{\dfrac{V_{i,j}}{n_{outref}}} \end{cases}$$

- The random noise attached to the average science pixels through pixel binning is

$$\sigma_{sub,bin} \approx \sqrt{\sigma_{sci,bin}^2 + \left(\frac{o\overline{f_i}+\overline{Q_i}}{\overline{Q_i}}\sigma_{onref,ave}\right)^2 + \sigma_{outref,ave}^2}$$

$$\approx \sqrt{\underbrace{\left(\overline{g_j} o\overline{f_i} + \overline{g_j}\overline{Q_i}\right)}_{\text{photon noise}} + \underbrace{V_{i,j}}_{\text{dark current}})n_{sci} + \underbrace{\left(\frac{o\overline{f_i}}{\overline{Q_i}}\right)^2 \frac{\overline{g_j}\overline{Q_i}+V_{i,j}}{n_{onref}} + \frac{V_{i,j}}{n_{outref}}}_{\text{reference pixel noise}}}$$

Example of transit curve without photon noise

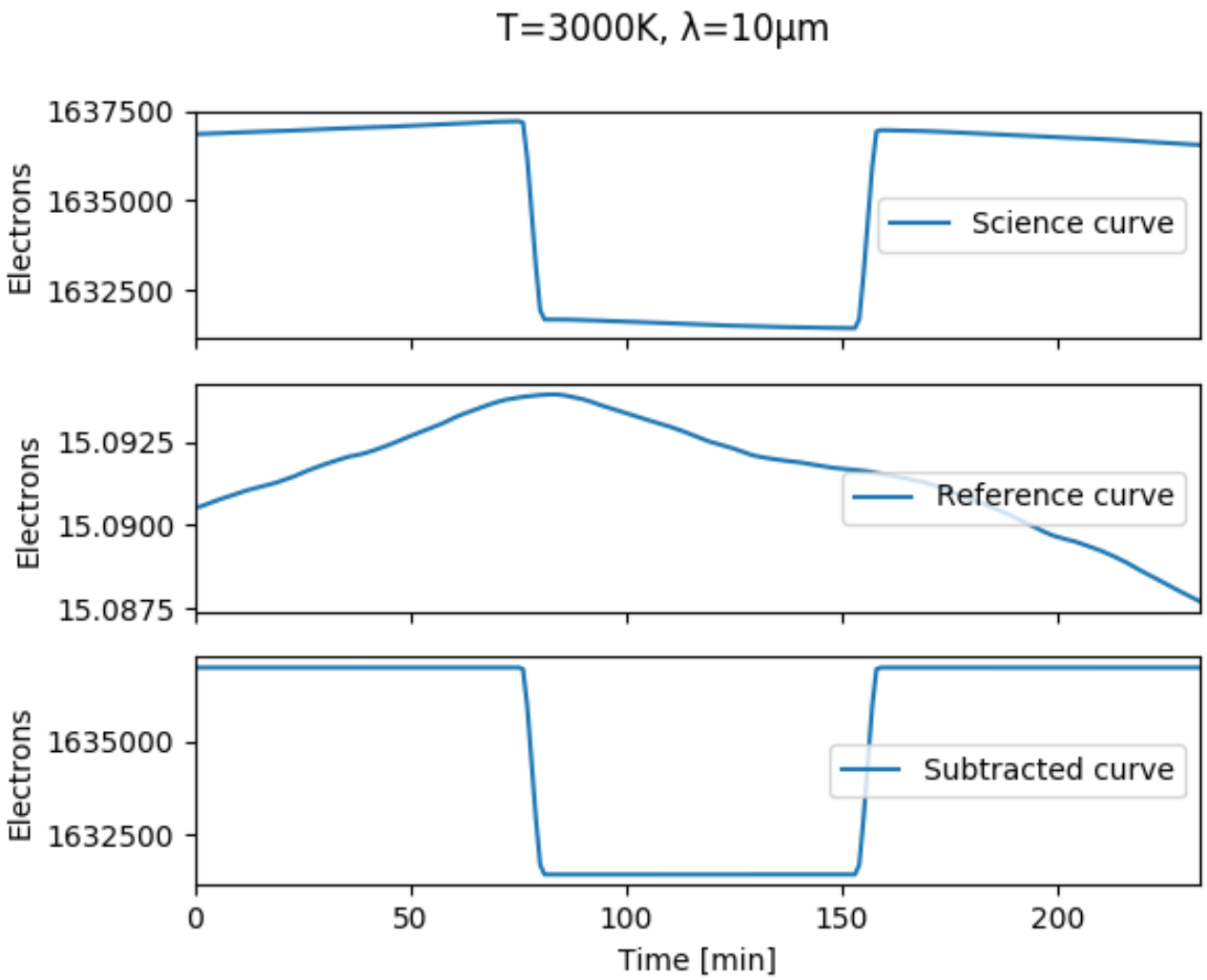

Photon noise: None
Dark current: 0.2 e-/sec
Readout noise: 14 e-
Peak-to-peak of gain fluctuation: 500ppm

Noise behavior for faint stars

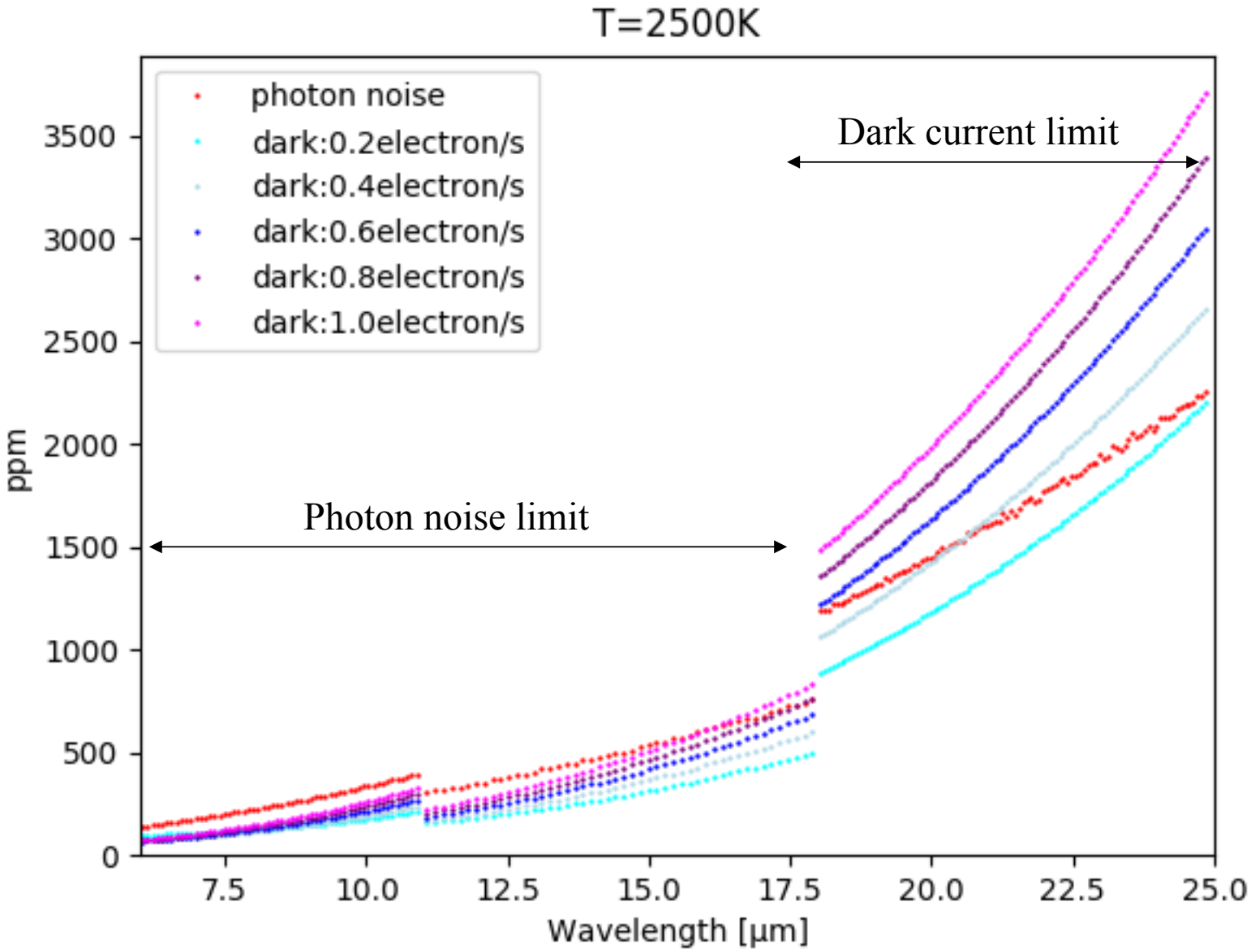

- Large dark current is dominant over the photon noise in the longer wavelength range.
- Small dark current (pale blue) is suitable for faint stars.

Noise behavior for bright stars

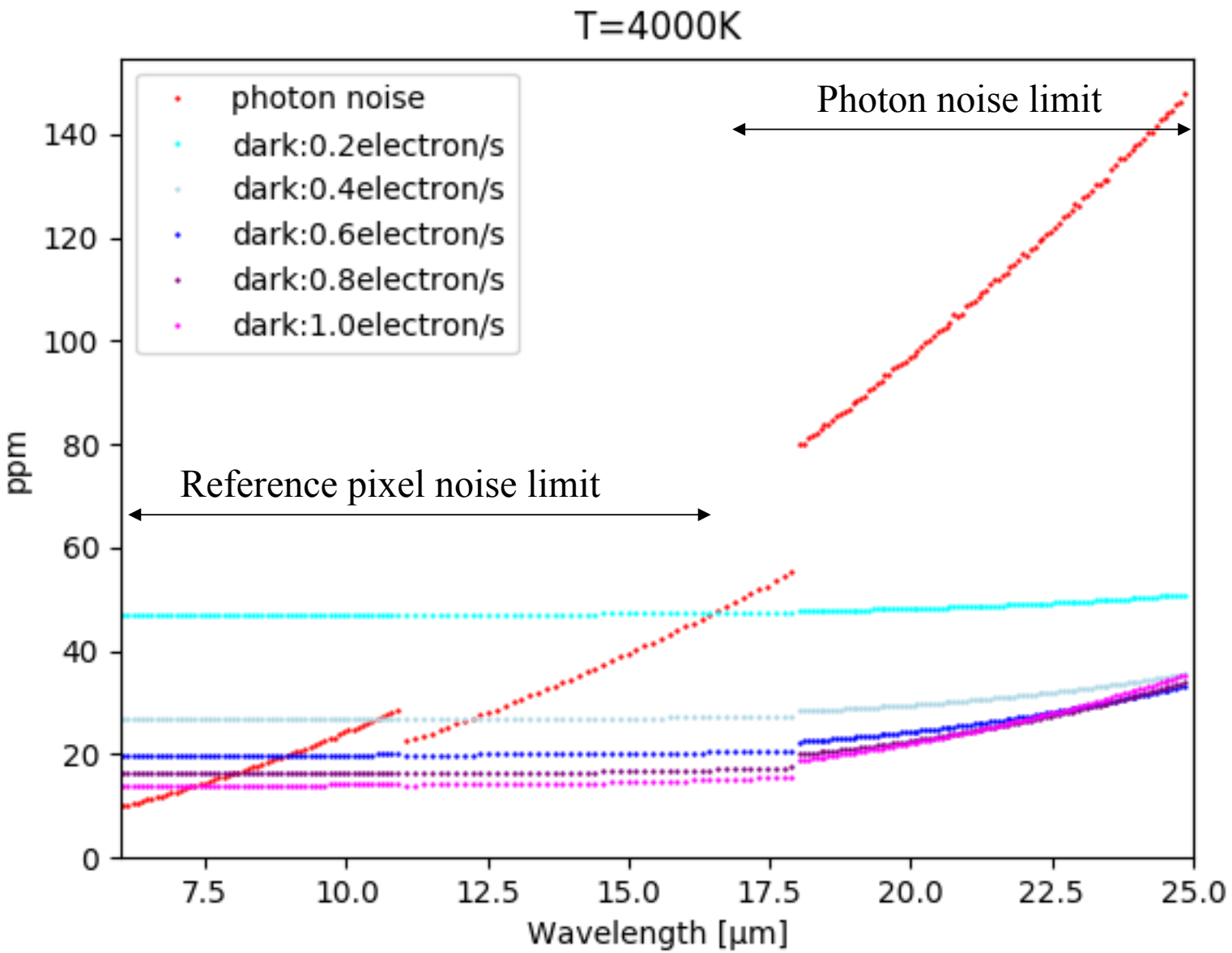

- Small dark current enhances the reference pixel noise and limits the sensitivity in the shorter wavelength range.
- Small dark current (purple) is suitable for bright stars.

Estimation error of transit depth

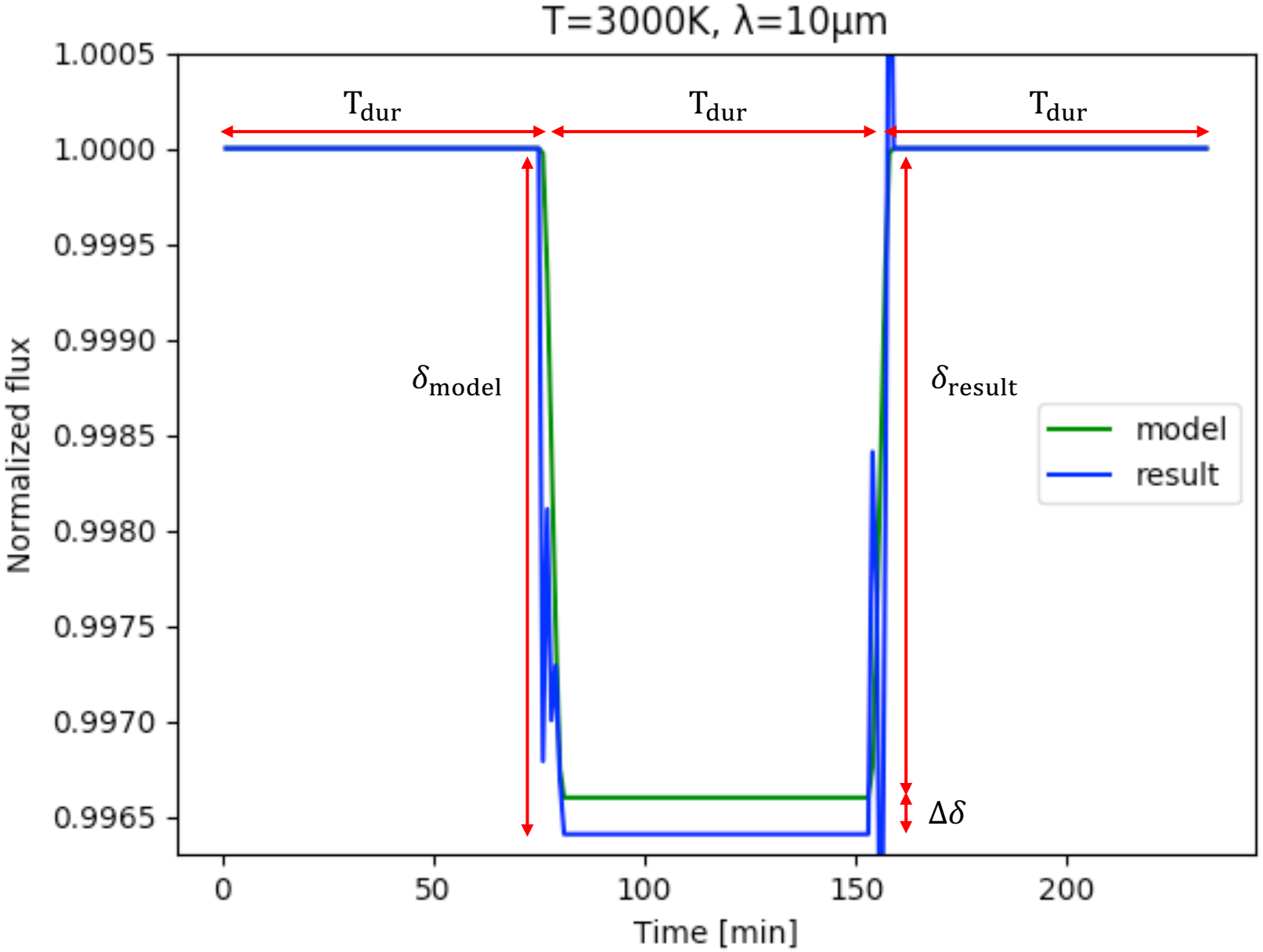

T_{dur}: transit duration
δ_{model}: input transit depth
δ_{result}: reconstructed transit depth

$$\Delta\delta = |\delta_{model} - \delta_{result}|$$

Uncertainty of reconstructed transit depth

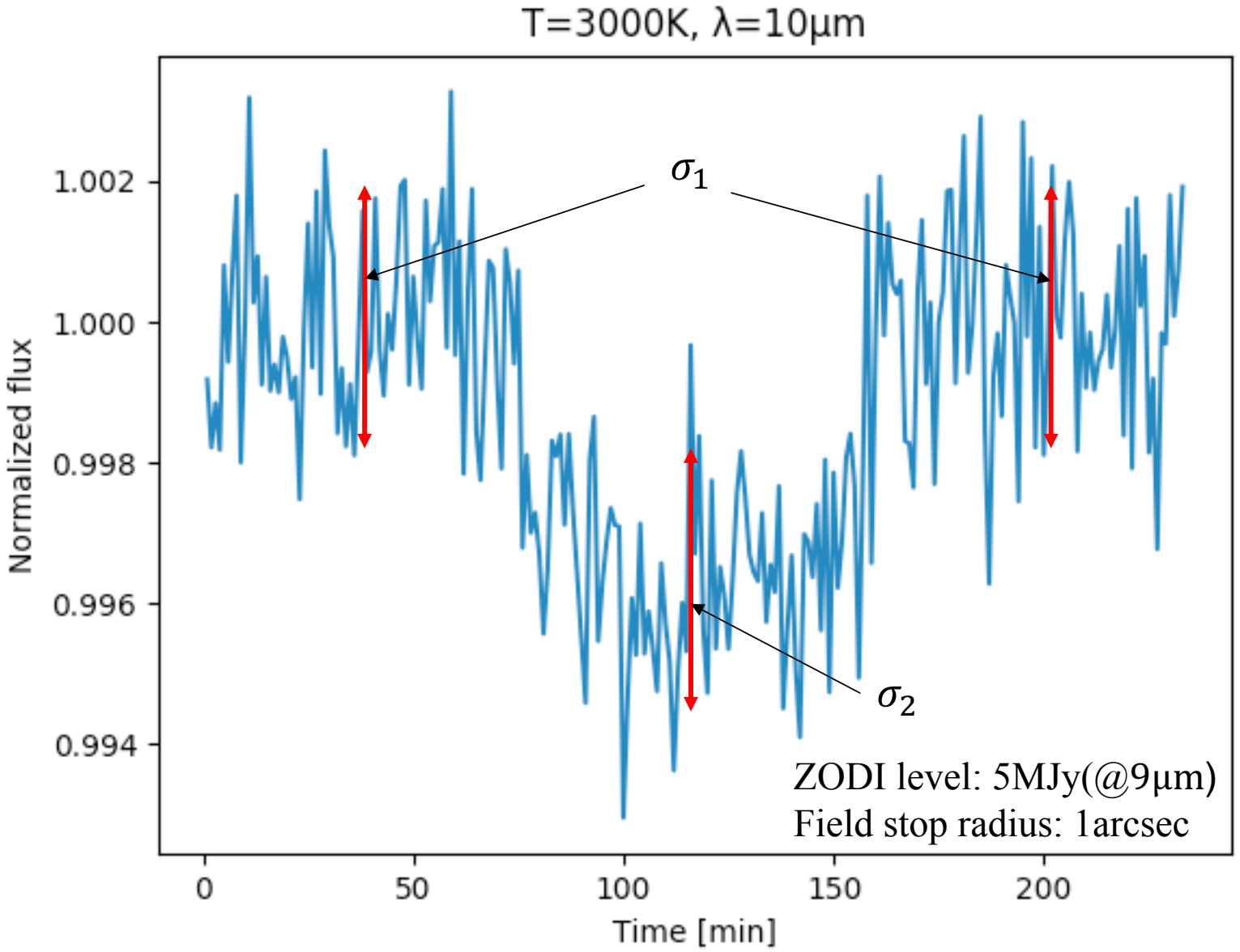

σ_1: RMS of continuum
σ_2: RMS of bottom in transit

$$\sigma = \sqrt{\sigma_1^2 + \sigma_2^2}$$

Derivation of estimation error and uncertainty

- Number of the calculations for each dot (one spectral element under a condition) is 100.
- Error attached to the measurement of transit depth is decomposed into deviation from the true depth (systematic error) and uncertainty (random error). The systematic error and uncertainty are calculated as follows:

$$\Delta\delta_{mean} = \frac{\sum_i^{100} \Delta\delta_i}{100},$$

$$\sigma_{mean} = \frac{\sum_i^{100} \sigma_i}{100}.$$

- Since the systematic noise is considered in this calculation, $\Delta\delta_{mean}$ and σ_{mean} are not comparable.
- The dots and error bars of the figures in pages 18-23 represent $\Delta\delta_{mean}$ and σ_{mean}, respectively.

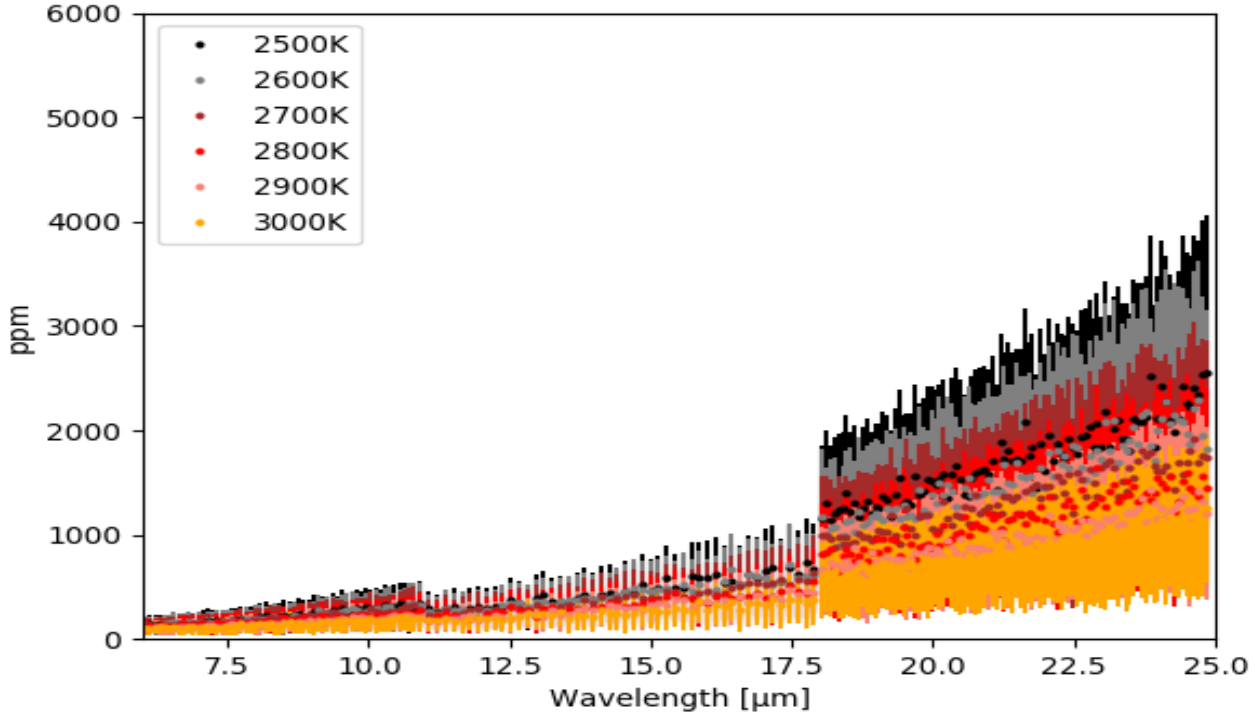

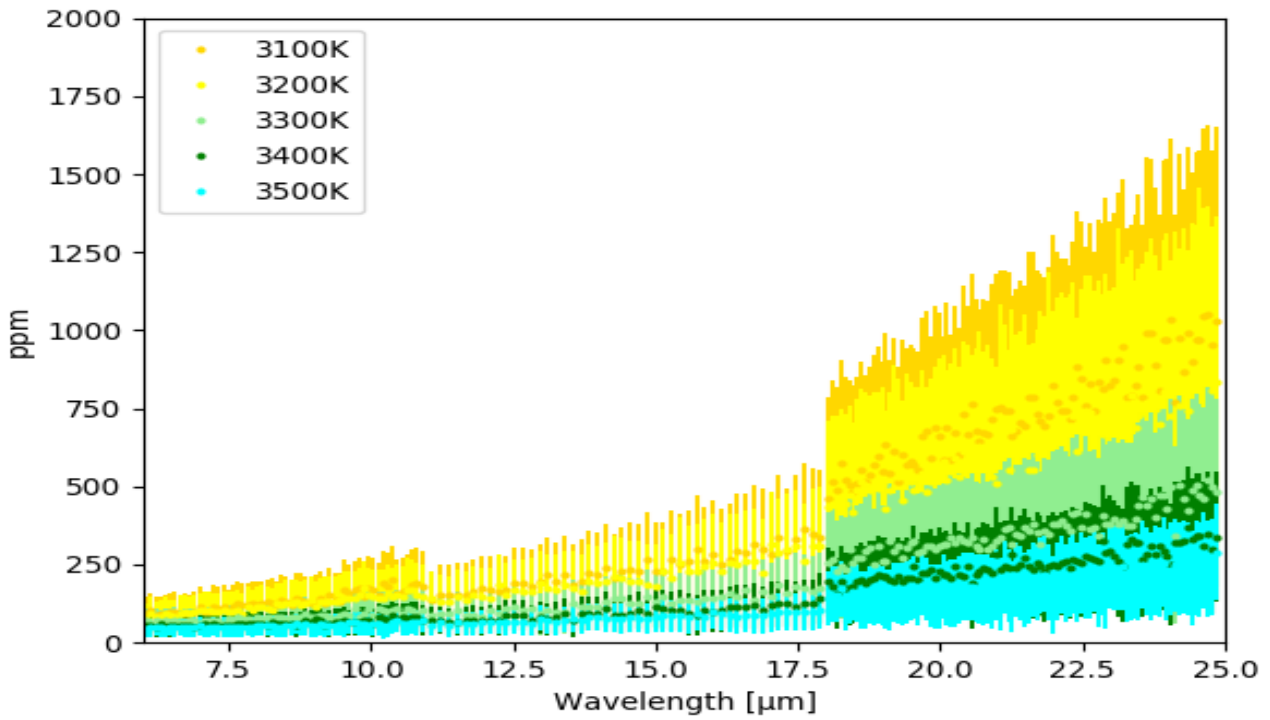

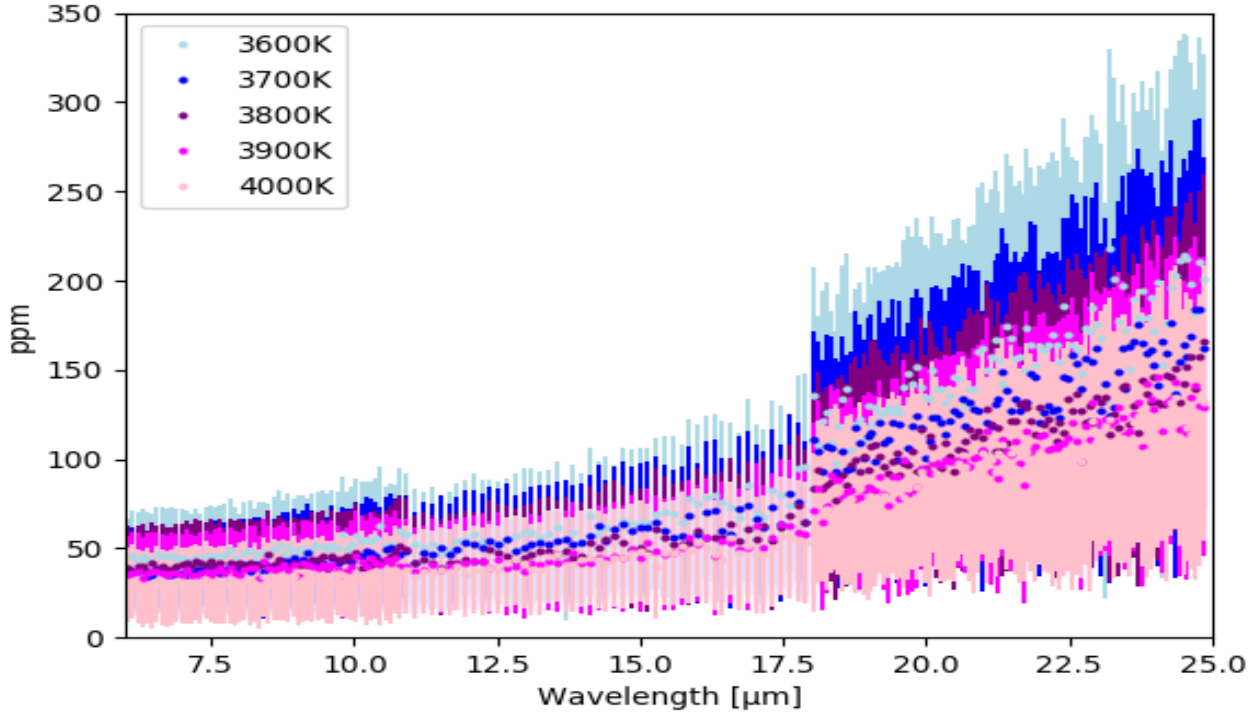

Calibration with reference pixels
Dark current: 0.2electrons/sec
ZODI level: 5MJy/sr (@9μm)
Field stop radius: 2arcsec

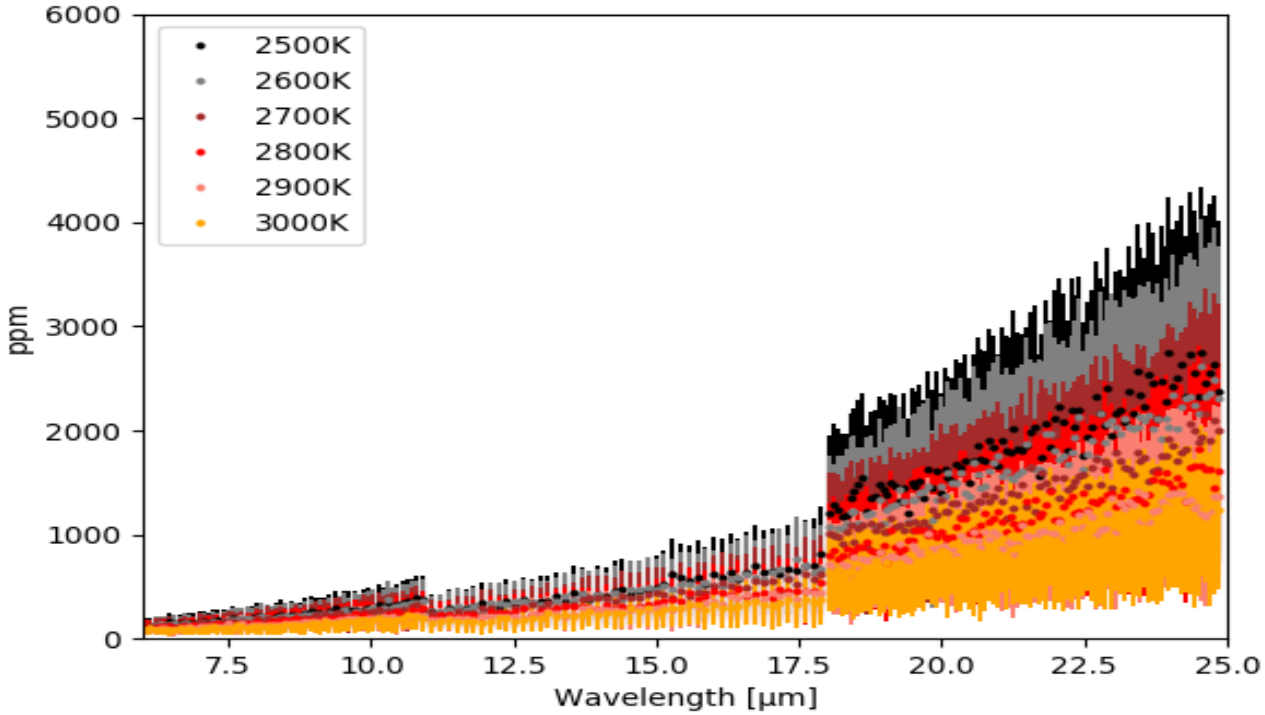

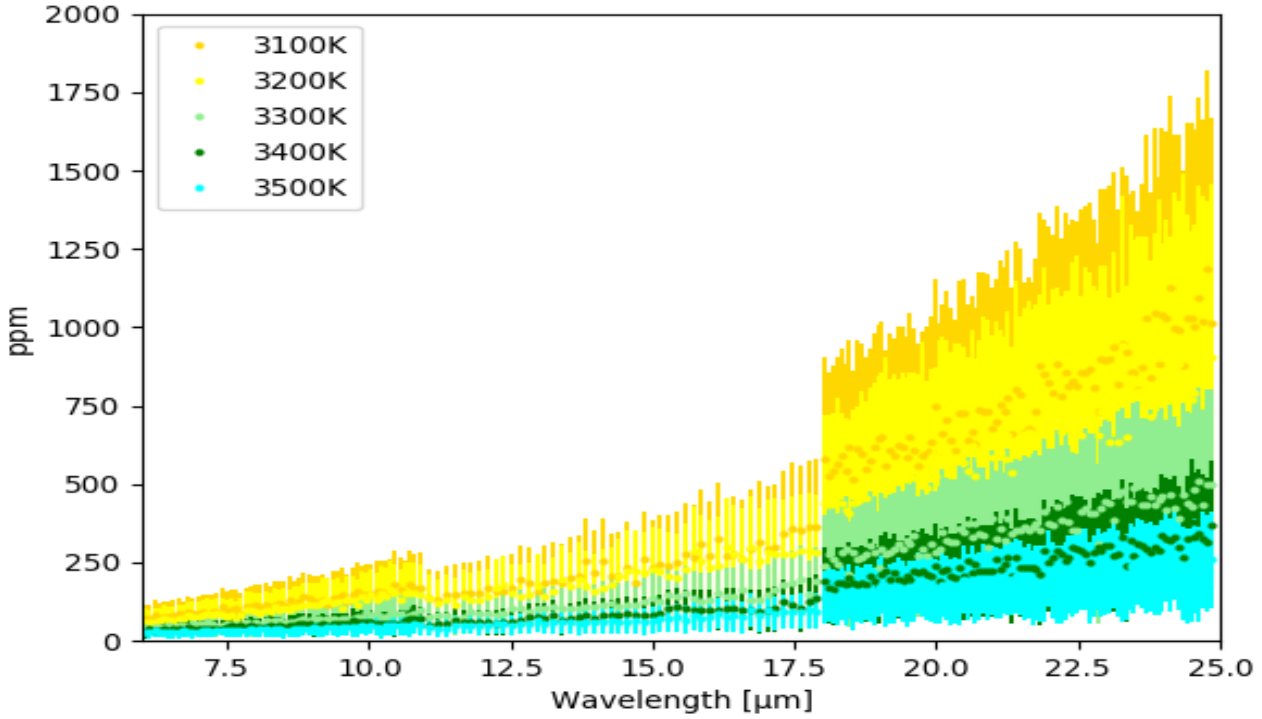

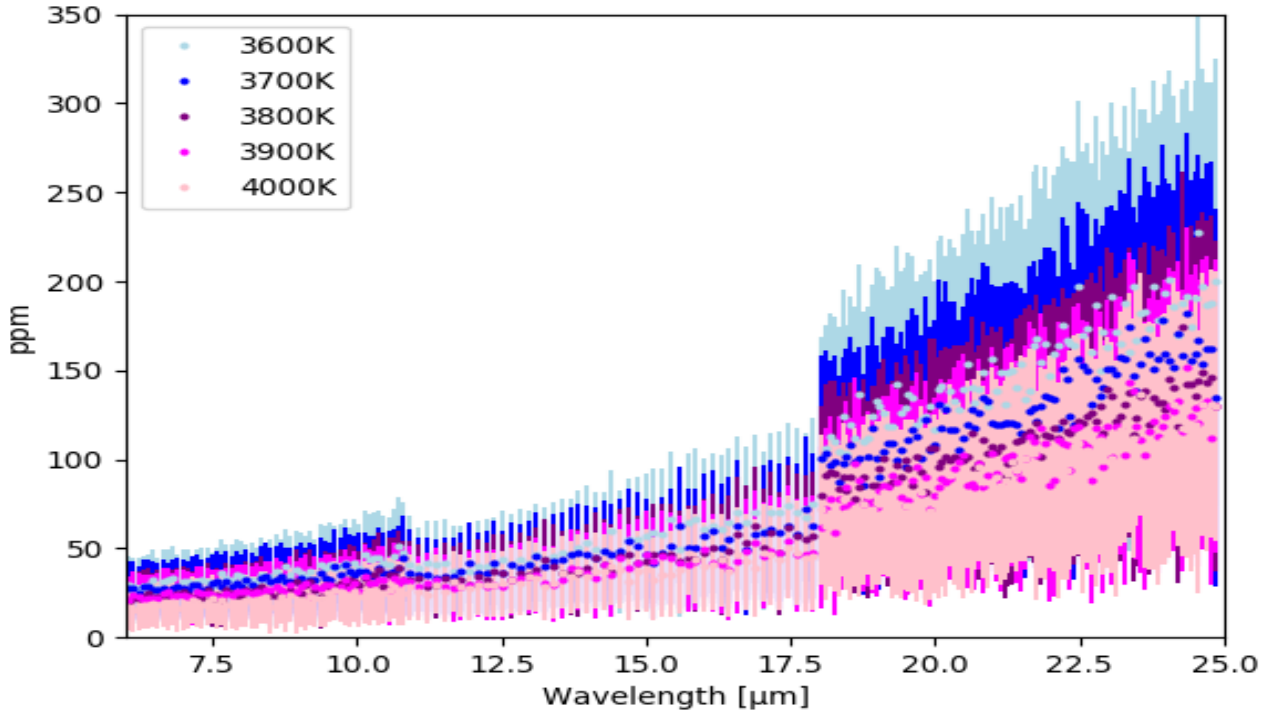

Calibration with reference pixels
Dark current: 0.4electrons/sec
ZODI level: 5MJy/sr (@9μm)
Field stop radius: 2arcsec

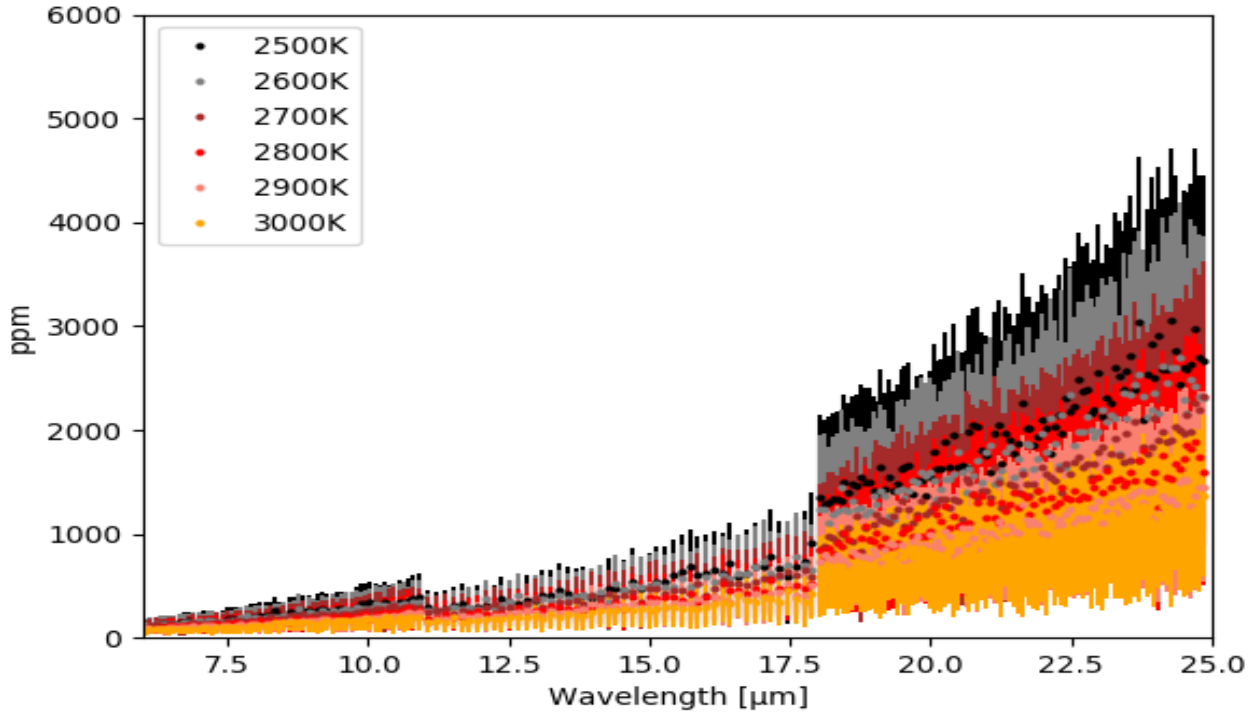

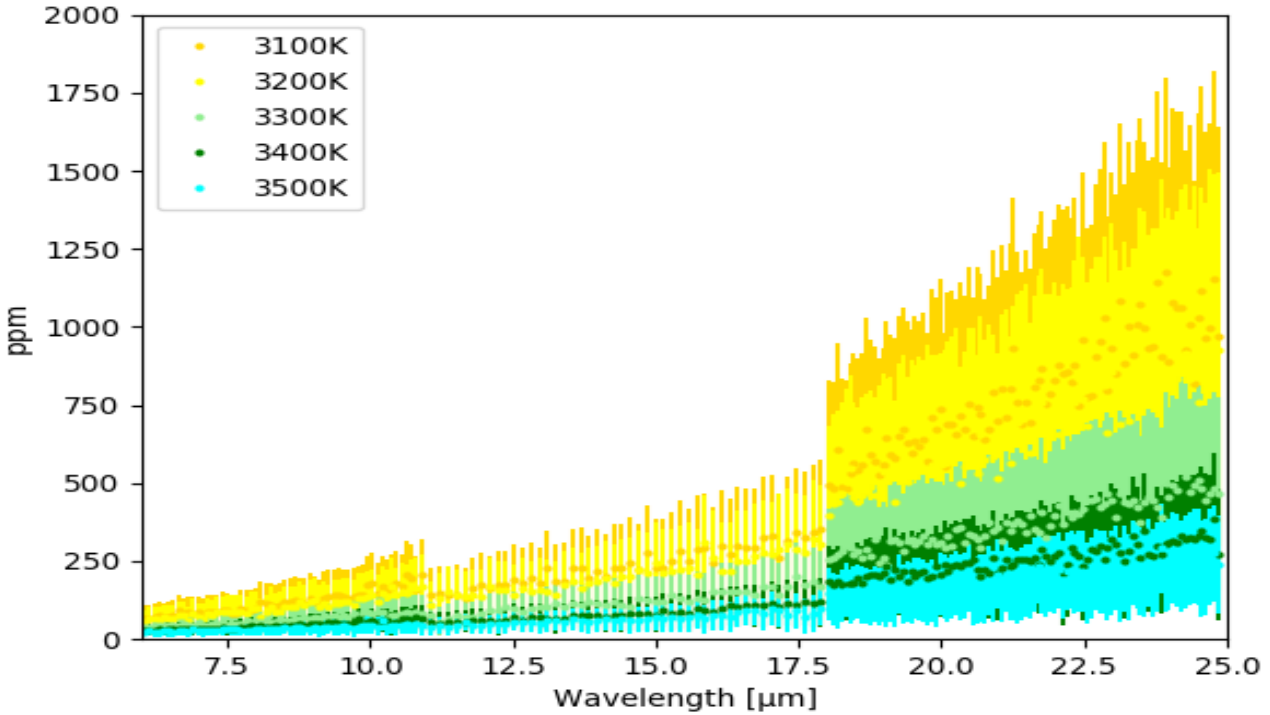

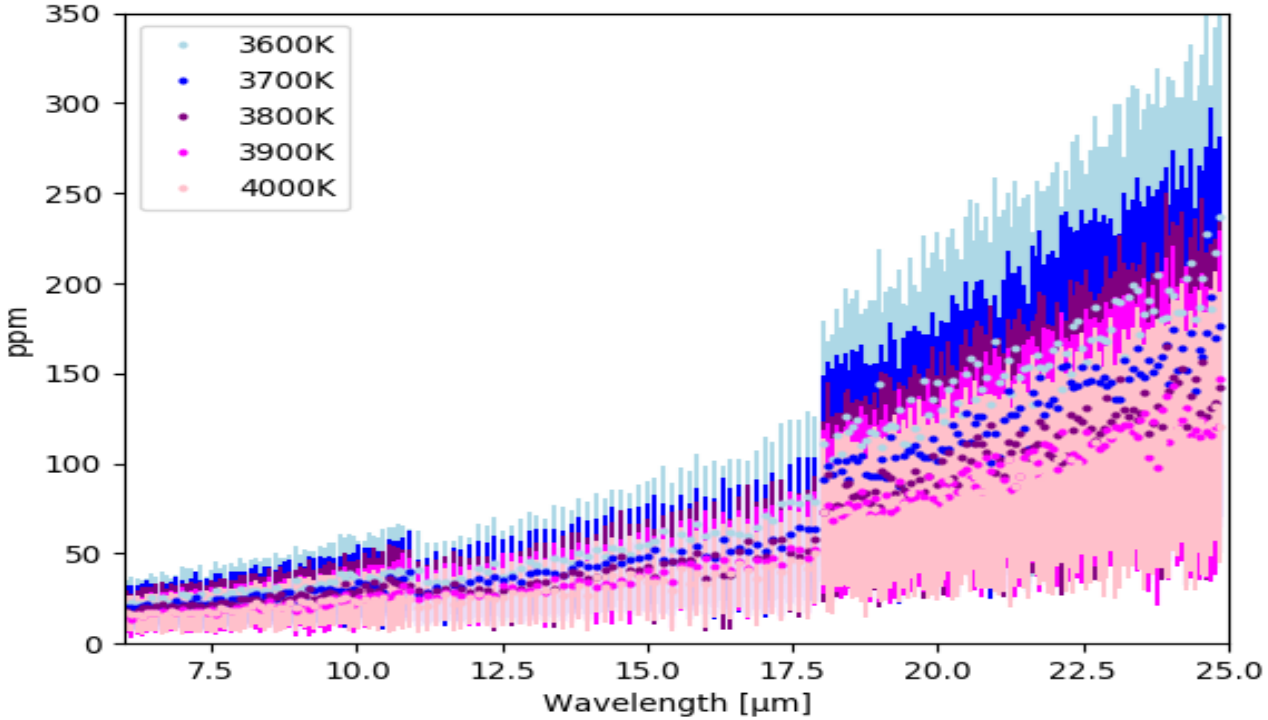

Calibration with reference pixels
Dark current: 0.6electrons/sec
ZODI level: 5MJy/sr (@9μm)
Field stop radius: 2arcsec

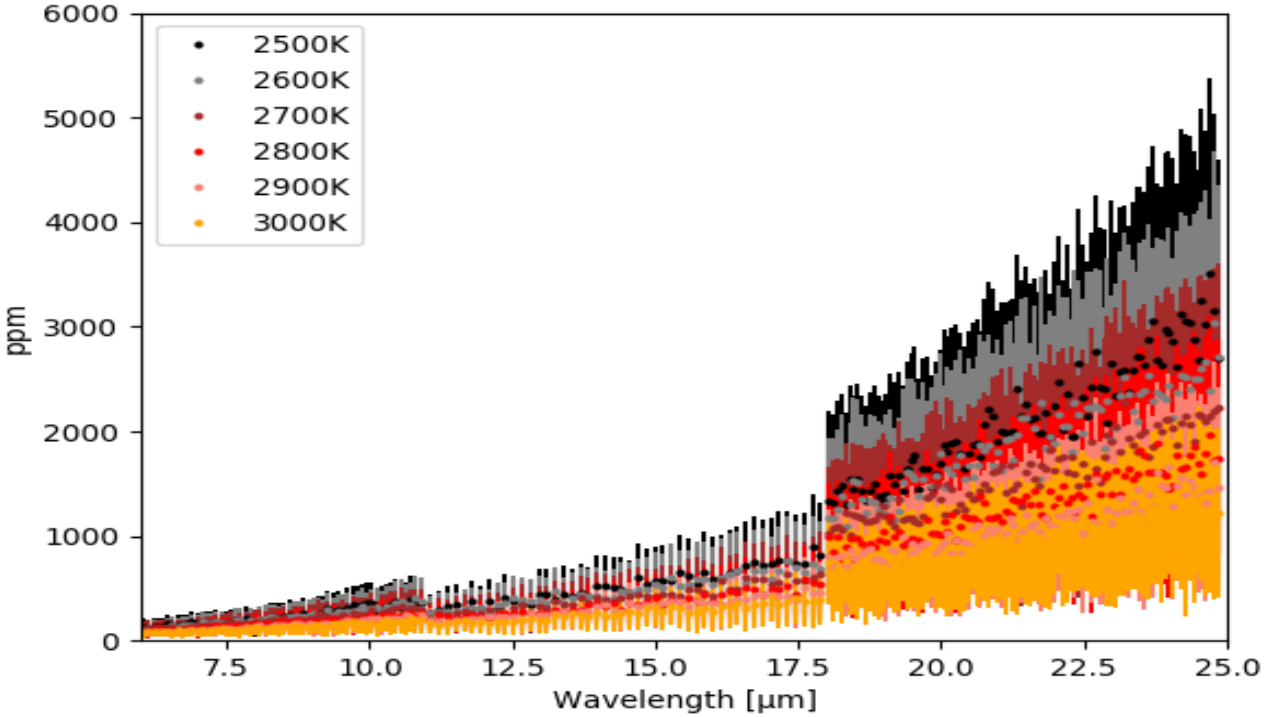

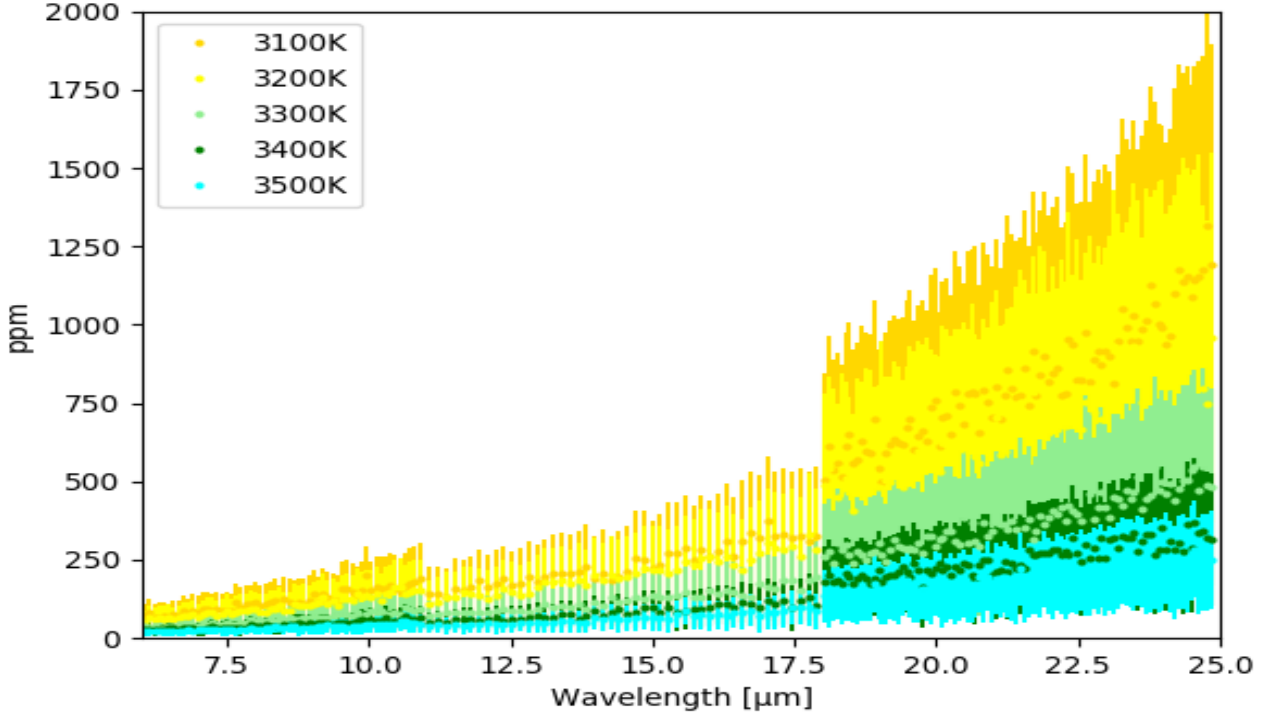

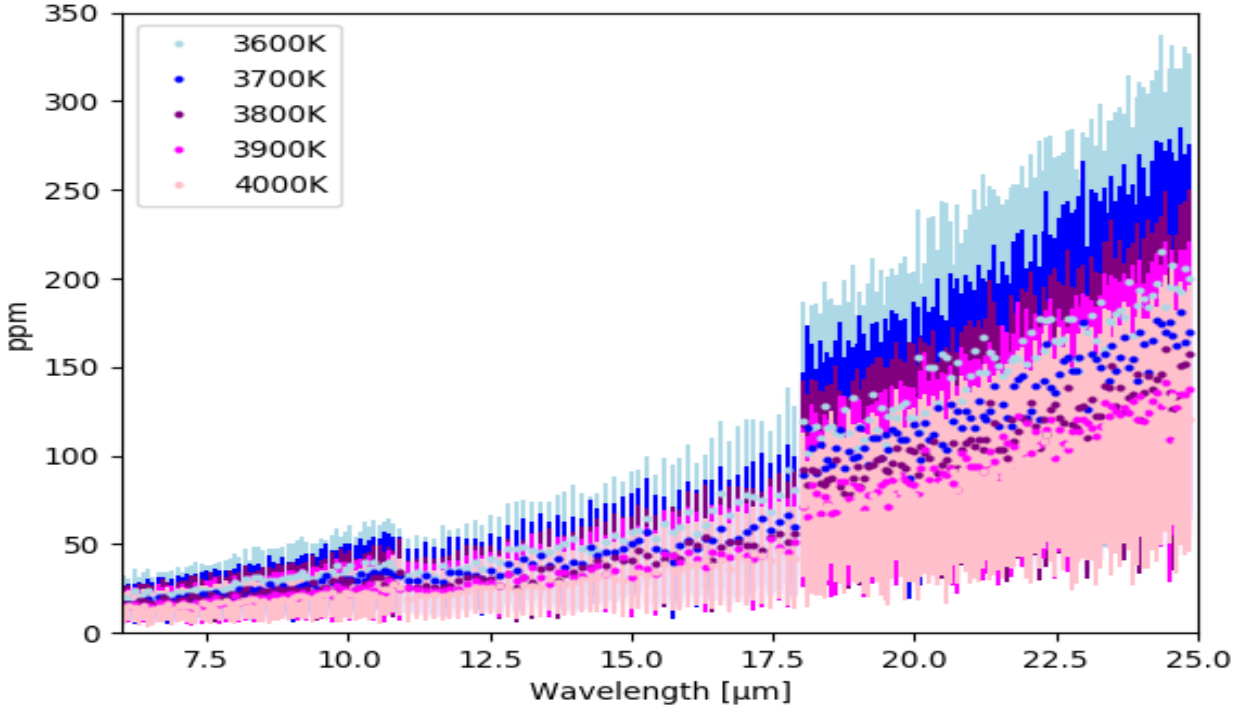

Calibration with reference pixels
Dark current: 0.8electrons/sec
ZODI level: 5MJy/sr (@9μm)
Field stop radius: 2arcsec

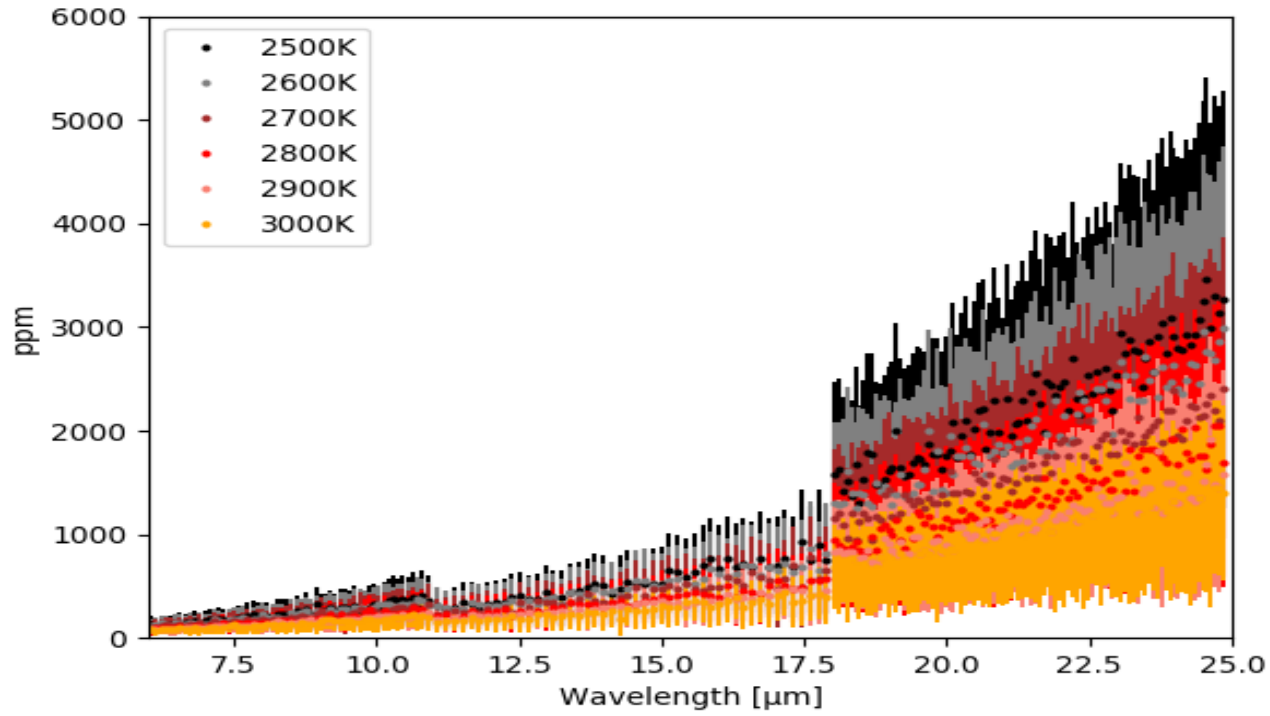

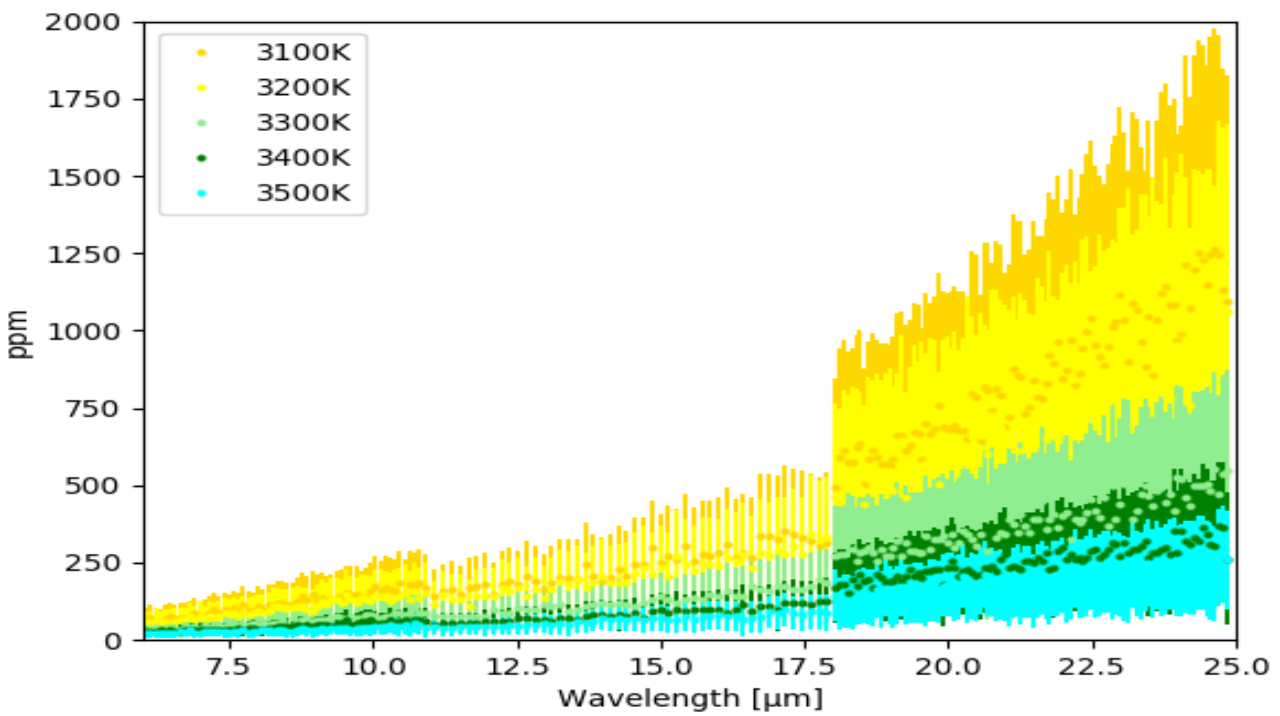

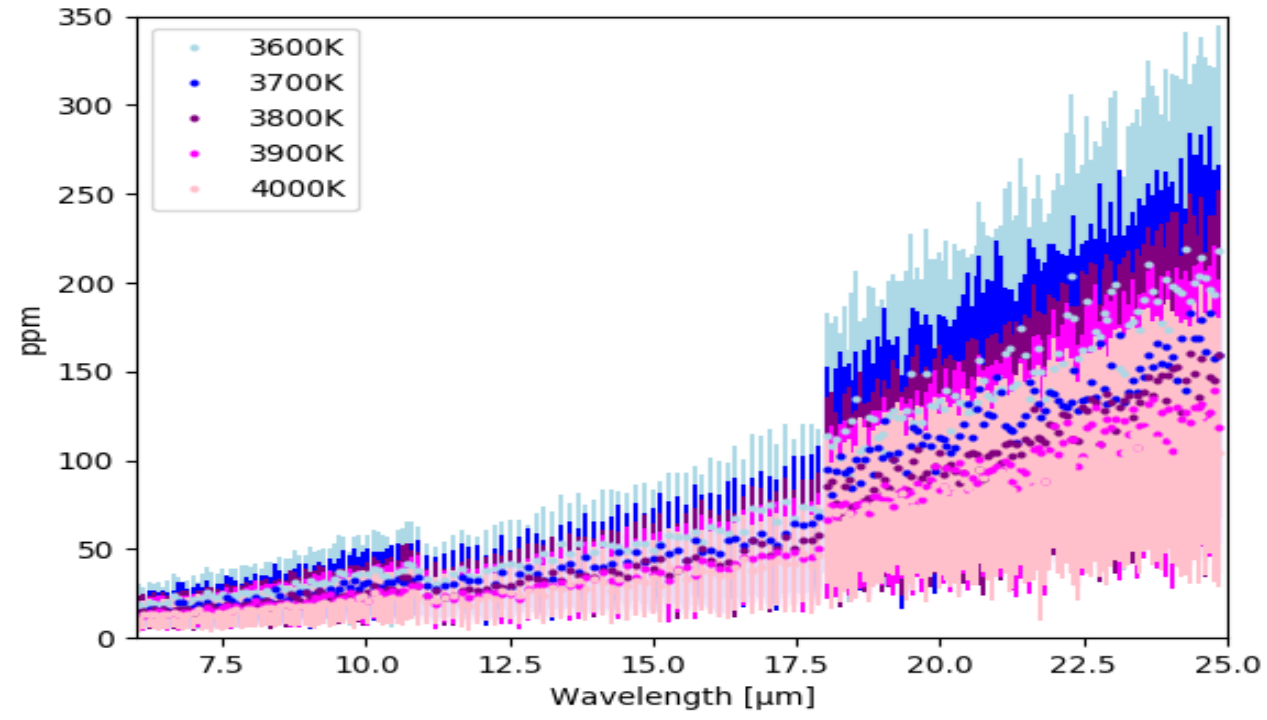

Calibration with reference pixels
Dark current: 1.0electrons/sec
ZODI level: 5MJy/sr (@9μm)
Field stop radius: 2arcsec

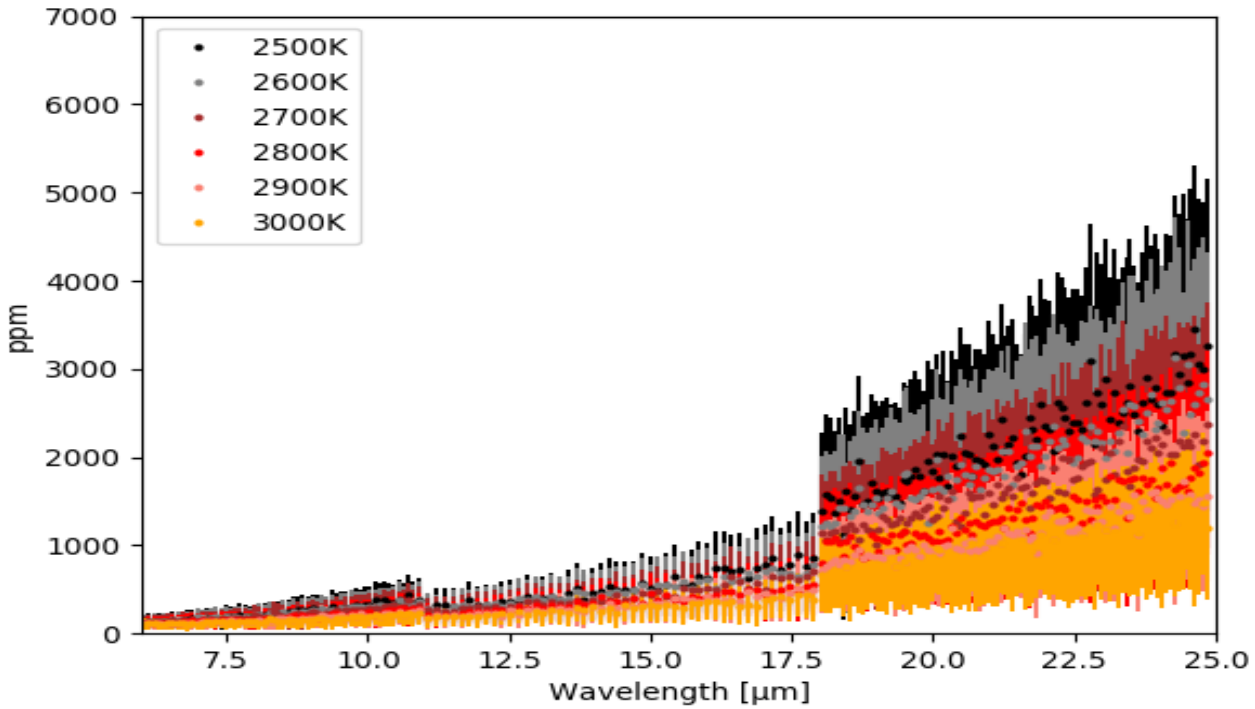

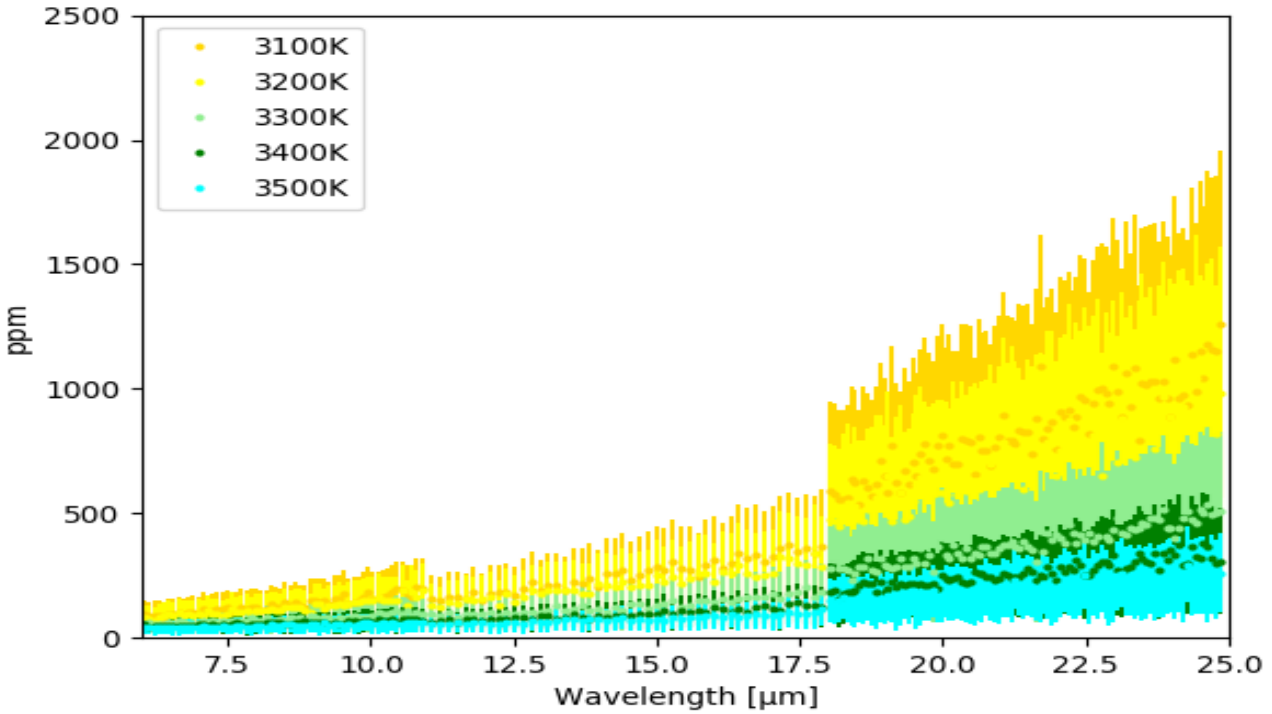

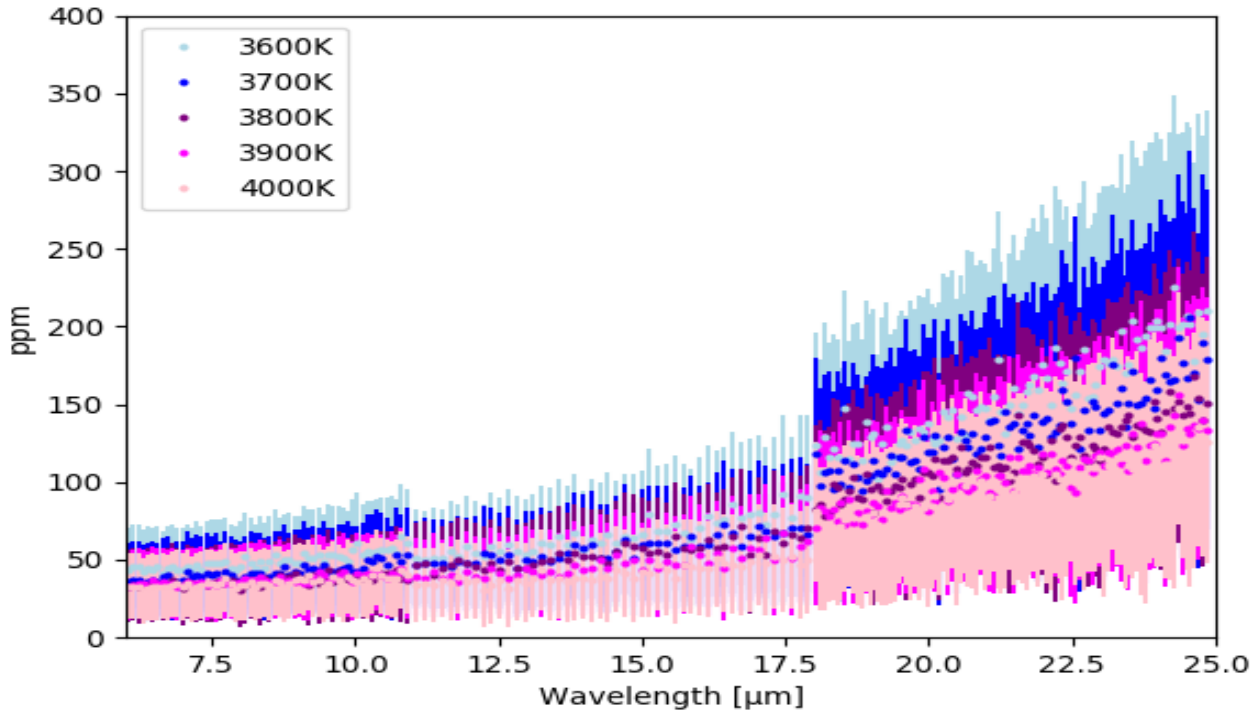

Calibration with reference pixels
Dark current: 0.2electrons/sec
ZODI level: 20MJy/sr (@9μm)
Field stop radius: 2arcsec